2007 | 2009 A

厚生労働科学研究費補助金

医療機器開発推進研究事業

がん特異的増殖機能を有するウイルス製剤と高感度GFP蛍光検出装置を用いた体外超早期がん診断および体内微小リンパ節転移診断システムに関する研究

(H17-ナノ-一般-04)

平成19年度　総括研究報告書

主任研究者　藤原　俊義

平成20（2008）年　4月

厚生労働科学研究費補助金（医療機器開発推進研究事業）
総括研究報告書

がん特異的増殖機能を有するウイルス製剤と高感度GFP蛍光検出装置を用いた体外超早期がん診断および体内微小リンパ節転移診断システムに関する研究

主任研究者　藤原　俊義

岡山大学医学部・歯学部附属病院
遺伝子・細胞治療センター・准教授

【研究要旨】
近年増加を続けるがん患者の生存率や治療成績の向上には、早期発見、適格な悪性度の予知、適切な治療方針の決定が重要な因子となる。特に、微小リンパ節転移の検出は患者のQOLを重視した必要最小限の低侵襲外科手術の確立に役立つ。

本研究では、テロメラーゼ活性（hTERT遺伝子発現）依存性にがん細胞で選択的に増殖し、オワンクラゲ由来の蛍光遺伝子GFP (Green Fluorescence Protein)を発現する改変アデノウイルス製剤 TelomeScan（Telomelysin-GFP、OBP-401）を標識薬剤とし、プローブ型の高感度GFP蛍光検出装置を用いた微小がん組織診断用の外科手術ナビゲーション・システムを開発する。TelomeScanを原発腫瘍内に局所投与することでリンパ流を経由するウイルスの所属リンパ節への拡散を促す。TelomeScanはリンパ節内の微小転移巣でがん細胞に感染・増殖して選択的にGFP蛍光を発するため、一定期間の後に転移リンパ節を可視化することができる。この技術により、微小リンパ節転移を手術中にリアルタイムに検出してリンパ節郭清範囲を同定する低侵襲外科手術が可能となる。最終年度となる平成19年度には、プローブ型高感度GFP蛍光検出装置の更なる改良と大動物における蛍光検出実験を計画した。

分担研究者：
田中　紀章
(岡山大学大学院医歯学総合研究科腫瘍制御学講座)
浦田　泰生
(オンコリスバイオファーマ・代表取締役社長)
永井　勝幸
(オンコリスバイオファーマ・神戸研究センター長)
河村　仁
(オンコリスバイオファーマ・事業開発部長)

A．研究目的

日本人の主要な死因が感染症から成人病、いわゆる生活習慣病へと移行する中で、特に癌は1981年以来日本人の死亡原因の第1位となっており、今後の本邦の癌罹患数は2015年には男性55万4000人、女性33万6000人となると推測されている。癌患者の生存率や治療成績の向上には、早期発見、適格な悪性度の予知、適切な治療方針の決定が重要な因子となる。特に、微小リンパ節転移の検出は患者のQOLを重視した必要最小限の低侵襲外科手術の確立に役立つ。

本研究では、テロメラーゼ活性依存性にがん細で選択的に増殖してオワンクラゲ由来の蛍光遺伝GFP (Green Fluorescence Protein)を発現する改変アデノウイルス製剤 TelomeScan (OBP-401)を標識薬剤とし、プローブ型の高感度GFP蛍光検出装置を用いた微小がん組織診断用の外科手術ナビゲーション・システムとしての有効性を検討する。1年目には、体外診断として末梢血中の浮遊がん細胞を検出する試みも平行して行っていたが、動物モデルにおいて体内リンパ節転移診断に関する良好な研究成果が得られた(**Kishimoto *et al*, *Nature Med.*, 12:1213-1219, 2006**)。したがって、より体内診断および低侵襲手術のための外科ナビゲーション・システムの開発が現実的となってきたため、以後は体内微小転移診断システムに重点をおいて研究開発を進めている。

微小リンパ節転移検出のためには、内視鏡などのアクセスを用いてTelomeScanを原発腫瘍内に局所投与することでリンパ流を経由するウイルスの所属リンパ節への拡散を促す。TelomeScanはリンパ節内の微小転移巣でがん細胞に感染・増殖して選択的にGFP蛍光を発するため、一定期間の後に開胸あるいは開腹にて転移リンパ節を可視化することができる。この技術により、微小リンパ節転移を手術中にリアルタイムに検出してリンパ節郭清範囲を同定する低侵襲外科手術が可能となる。肺がんや胃がんなどの進行固形がん手術の際に、TelomeScanはリンパ節内の微小転移巣で増殖しGFP蛍光を発するため、原発巣周辺の組織にプローブを接触させることで転移リンパ節を検出すること

目　　次

ができ、リンパ節廓清範囲決定の有効な指標となると期待される。また、胸膜あるいは腹膜播種病巣の検出には、胸腔や腹腔などの体腔内にTelomeScanを投与し、同様に一定期間の後に高感度GFP蛍光検出装置にて観察する。微小播種巣では選択的にTelomeScanが感染・増殖するため、肉眼では検出できない微小病巣を確認することができる。本技術は肉眼的に確認できない微小播種病巣を検出する診断用システムとして応用できることで、効果的な先進治療の開発が期待される。

B．研究方法

1）TelomeScan (OBP-401)の構造

TelomeScanは幼児の「かぜ」症状の原因となるアデノウイルス5型を基本骨格とし、テロメラーゼ構成成分であるhTERT (human telomerase reverse transcriptase)遺伝子のプロモーターの下流にウイルス増殖に必須のE1AおよびE1B遺伝子がIRES配列で連結して組み込まれている。また、ウイルスゲノムのE3領域に、サイトメガロウイルス（CMV）プロモーターとオワンクラゲ由来のGFP (Green Fluorescent Protein)蛍光発現遺伝子が挿入されている（図1）。TelomeScanは癌細胞で選択的に増殖し、GFP蛍光を発するとともに、最終的には細胞死を誘導する。一方、テロメラーゼ活性を持たない正常細胞では、その増殖は抑制され、GFPもみられず、細胞死も生じることはない。

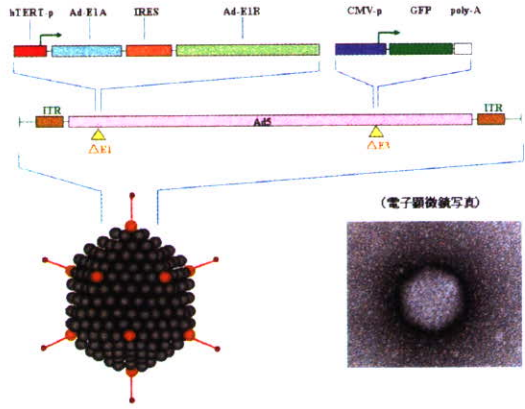

図１　**TelomeScanの構造と概観**

2）プローブ型高感度蛍光検出装置の試作

前年度に作成した第1号試作機は、プローブ内にレンズとモノクロCCDカメラ、および蛍光励起のためのLEDを内蔵したため、7（縦）x 7.5（横）x 29（長さ）センチとサイズ的にかなり大型のものとなった。同機でマウス直腸がんリンパ節転移を開腹下に観察したところ、正常組織による自家蛍光がかなりのノイズとなることが判明したため、画像解析ソフトの蛍光検知閾値を調整することで転移リンパ節のみを高感度に検知することが可能となった。しかし、サイズと重量が著しくプローブの操作性を損なっているため、励起光を独立させて術野に照射する案も検討したが、その場合は部屋を暗室状態にする必要があり、現実的ではないと判断した。そこで第2号試作機では、プローブにはレンズとLEDのみを内蔵し、イメージファイバーでつないだ本体にカラーCCDカメラを設置する方法を採用した。さらに、ファイバーを軽量化して柔軟性を持たせ、撮像面積も広げた第3号試作機も作成した。

3）大動物によるプローブ型高感度蛍光検出装置の機能検証

試作機を用いて大動物での実験を考えたが、担がん大動物を実験的に準備することは困難であるため、まずTelomeScanと同様の蛍光を発する蛍光ビーズを調達した。直径50 nmから500 nmまでの各種サイズのFluoresbrite Carboxylate Microspheres（フナコシ）を準備した。

東京農工大腫瘍科の伊藤博教授との共同研究で、飼主の同意を得た上で、担がんイヌの手術の際に蛍光ビーズを患部に注入し、所属リンパ節を蛍光にて確認しながら切除を行うセンチネル･ナビゲーション手術を試みた。

（倫理面への配慮）

制限増殖機能を有するTelomeScanを用いる本研究は「大臣確認実験」となるため、「第二種使用等拡散防止措置確認申請書」を作成、学内の担当部署での検討の後に文部科学省に申請し、研究計画実施の承認を得ている。

C．研究結果

1）プローブ型高感度蛍光検出装置の試作

第2号試作機では、プローブにはレンズとLEDのみを内蔵し、イメージファイバーでつないだ本体にカラーCCDカメラを設置することで、5（縦）x 5（横）x 17.4（長さ）センチとプローブの小型化、軽量化が実現した（図2a）。また、プローブ外筒を滅菌対応とすることで清潔操作も可能となった。さらに、フットスイッチにより画像キャプチャーを簡便化し、片手で操作可能とした（図2b）。

ただ、イメージファイバーが剛性を有しているため、操作性はやや不良であり、撮像視野面積（径3.6mm）が狭い点が欠点であった。

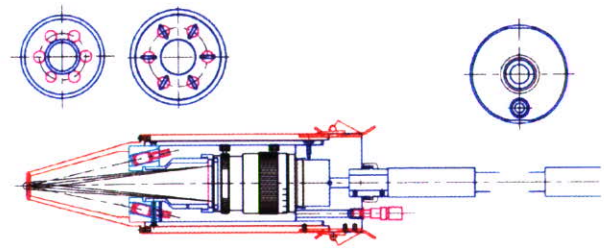

図2a　第2号試作機プローブの構造図

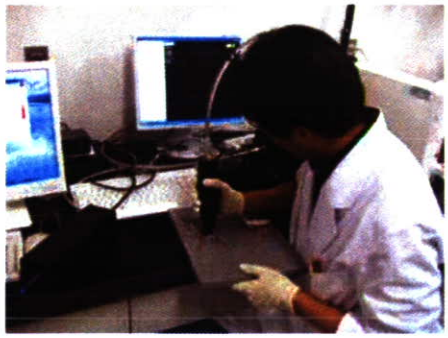

図2b　第2号試作機プローブの実験風景

また、画像解析ソフトで微弱な蛍光を色別に表示するカラーディスプレイを採用したことで、極めて容易に蛍光部位を同定することができた（図2c）。実際に、ヌードマウスの背部に移植したヒト大腸がん皮下腫瘍、および同所性に移植したヒト大腸がんの傍大動脈リンパ節転移を高感度に検出することが可能であった。

図2c　画像解析ソフトによる高感度蛍光検出

第2号試作機の問題点は、ファイバーの剛性が操作性を損なっていることと、撮像視野面積が径3.6mmと小さく、臨床応用の際のスキャン範囲が限られることであった。そこで、さらにファイバーを軽量化して柔軟性を持たせ、撮像面積も約4倍（径6.6mm）に広げながらも34万画素の高解像度を維持した第3号試作機を作成した（図3a）。ファイバー形状が金属ブレードからPVCチューブとなることで剛性が消失し操作性が向上した（図3b）。

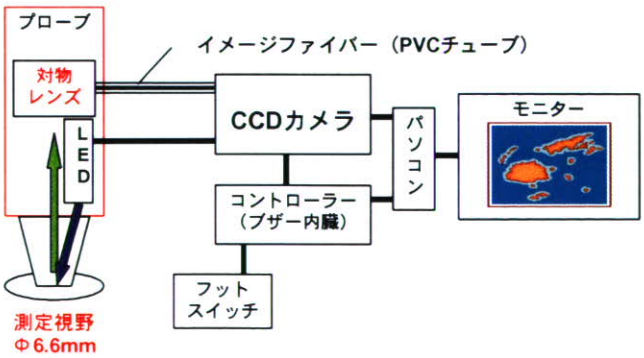

図3a　第3号試作機のシステム図

図3b　プローブ先端と柔軟なファイバー

マウスを用いた実験では操作性とスキャン範囲は格段に向上しており、2号機と同様の感度で転移リンパ節を描出することが可能であった（図3c）。

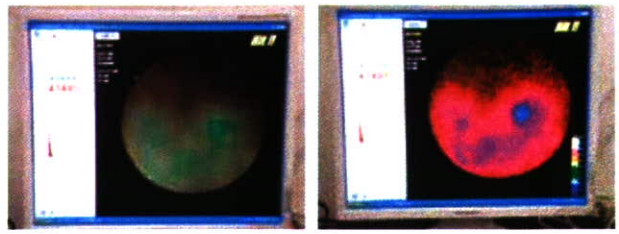

図3c　エッジ処理による高感度蛍光検出

3）大動物によるプローブ型高感度蛍光検出装置の機能検証

手術野での清潔操作のために、脱着式プローブ外筒を前日ガス滅菌した。術野で細長い滅菌プラスチックバックに清潔な外套を入れ、バックの端をカットしてプローブ先端の接触部を出し、清潔な粘着テープにてプローブ外筒とプラスチックバックを固定した。次いで、プローブ本体をプラスチックバックの内側から外筒に装着し、術野操作に備えた（図4a）。

図4a　清潔なプローブ先端と蛍光ビーズ

右第5乳腺の腫瘍を持つ雑種犬に、全身麻酔下に腫瘍周辺に50 nmおよび200 nmの蛍光ビーズを注入した（図4b）。15分後に体表から頭側に向かって流れるリンパ流に沿ってリンパ節を観察したところ、蛍光強度は弱かったものの、位置を確認することができた（図4c）。治療は両側5個ずつの乳腺をすべて摘出する手術となるので、切除の際の皮膚切開部からプローブを当てるとより鮮明に描出可能であった。さらに、切除標本で強い蛍光を発

するリンパ節を感知することができ、切除部位にリンパ節の遺残がないことも確認できた。50 nmの蛍光ビーズの方が所属リンパ節への到達速度が速く、30分後にはきわめて鮮明に検出可能であった。

図4b　乳腺患部への蛍光ビーズの注入

図4c　体表からの蛍光観察

図4d　切開創からのリンパ管描出

図4e　切除標本でのリンパ節確認

前肢骨肉腫のGレトラバーの断脚に際して同様の実験を行い、所属リンパ節を鮮明に描出することが可能であった。すなわち、大動物を対象とした本実験によって、検出機器の感度と操作性を確かめることで臨床での有用性について検証することができたと考える。

D．考察

ウイルスは本来ヒトの細胞に感染して、その構造蛋白質を産生することで複製・増殖する。その増殖機能に選択性を付加することにより、がん細胞を標識する診断用製剤として用いることが可能となる。「かぜ」症状の原因となるアデノウイルス5型を基本骨格とするTelomeScanは、ウイルス増殖に必須のE1遺伝子をテロメラーゼ構成分子であるhTERT (human telomerase reverse transcriptase)遺伝子のプロモーターで制御することで、がん細胞のみで増殖するように改変されたウイルス製剤である。さらに、E3領域にGFP遺伝子が組込まれており、がん細胞のみで緑色蛍光を発する。

われわれが標的とするテロメラーゼは80-90%の癌で極めて高い活性の上昇がみられ、正常組織で活性が検出されるリンパ球や小腸上皮での発現レベルは低いため、TelomeScanのがん選択性はかなり厳格かつ広範である。また、TelomeScanはがん細胞で複製・増殖するため、経時的なGFP蛍光強度の増強が期待できることが画期的であり、ウイルスを細胞標識に用いる点が独創的であると言える。さらに、GFPは導入遺伝子発現などの目的で多くの基礎研究で使用されているため、蛍光顕微鏡やFACSなどの検出技術の開発が進んでおり、TelomeScanのGFP蛍光を高感度に検出する装置の開発は技術的には可能と思われる。

本年度までの研究で、TelomeScanを原発腫瘍内に局所投与することで、リンパ流を経由するウイルスの所属リンパ節への拡散を促すことができた。また、TelomeScanはリンパ節内の微小転移巣でがん細胞に感染・増殖して選択的にGFP蛍光を発するため、マウスモデルにおいては一定期間の後に転移リンパ節を可視化することが可能であった。本年度は、プローブ型高感度GFP蛍光検出装置の第3号試作機によって、マウスモデルおよび大動物モデルにおいて、TelomeScanと同様の緑色蛍光を発する蛍光ビーズを操作性よく、かつ高感度に検出・観察することが可能であった。

平成18年10月から米国ダラスにて、米国食品医薬品庁（FDA）の承認のもと、TelomeScanとGFP発現カセット以外の基本骨格を同じくする抗がんウイルス製剤 Telomelysinの臨床試験が行われており、その安全性が確認されつつある。この安全性情報は、今後のTelomeScanの臨床研究計画の立案に極めて有用な根拠となると期待される。

しかし、本技術を開発してきた3年間に、胃がんや肺がんなどの外科治療の主体が開腹・開胸手術から鏡視下手術へと急速に移行してきた。そこで

今後は、プローブによる転移リンパ節検出を目指す本技術の対象を、センチネル・ナビゲーションが日常診療に用いられている乳がん、あるいは体表からの検出が有効な肉腫系手術に集約し、臨床的有用性を検討していく。センチネルリンパ節はリンパの流れを示すのみで、転移リンパ節特異的な描出が可能なわけではないため、本技術により転移リンパ節そのものを検出することができれば、リンパ節廓清範囲決定の有効な指標となると期待される。

E．結論

テロメラーゼ活性依存性に癌細胞で選択的に増殖して蛍光遺伝子GFPを発現する改変アデノウイルス製剤TelomeScanは、標識薬剤として微小リンパ節転移検出外科手術ナビゲーション・システムに応用可能であり、高感度にその蛍光を検出するプローブ型検出器を開発することができた。

F．研究発表

1. 論文発表

【英文】

1. Endo, Y., Sakai, R., Ouchi, M., Onimatsu, H., Hioki, M., Kagawa, S., Uno, F., Watanabe, Y., Urata, Y., Tanaka, N., and Fujiwara, T. Virus-mediated oncolysis induces danger signal and stimulates cytotoxic-T-lymphocyte activity via proteasome activator upregulation. ***Oncogene*** 2007; (in press).
2. Hashimoto, Y., Watanabe, Y., Shirakiya, Y., Uno, F., Kagawa, S., Kawamura, H., Nagai, K., Tanaka, N., Kumon, H., Urata, Y., Fujiwara, T. Establishment of Biological and Pharmacokinetic Assays of Telomerase-Specific Replication-Selective Adenovirus (TRAD). ***Cancer Sci.*** 2008; 99, 385-390.
3. Fujiwara, T., Urata, Y., Tanaka, N. Telomerase-specific oncolytic virotherapy for human cancer with the hTERT promoter. ***Curr. Cancer Drug Targets*** 2007; 7: 191-201.
4. Fujiwara, T., Urata, Y., Tanaka, N. Diagnostic and therapeutic application of telomerase-specific oncolytic adenoviral agents. ***Front. Biosci.*** 2008; 13: 1881-1886.

【邦文】

1. 藤原俊義、田中紀章：GFP 発現ウイルス製剤を用いた消化器癌微小転移の *in vivo* イメージングシステム. *医学のあゆみ* 2007; 220: 659-661.
2. 藤原俊義、田中紀章：癌のウイルス療法. *外科治療「腫瘍外科治療の最前線」* 2007; 96 Suppl.: 368-373.
3. 藤原俊義、田中紀章：テロメラーゼ特異的ウイルス製剤の癌診断・治療への応用. *ゲノム医学* 2007; 7: 129-134.
4. 藤原俊義、田中紀章：テロメラーゼ依存性腫瘍融解ウイルス製剤のがん診断・治療への応用. *日本臨床* 2007; 65: 1913-1922.
5. 藤原俊義：ナノバイオ・ウイルス製剤のがん診断への応用. ***Medical Bio*** 2007; 4: 39-43.
6. 藤原俊義、田中紀章：p53 遺伝子を発現するアデノウイルスベクターを用いた肺癌の遺伝子治療（平成 18 年度岡山医学会賞（林原賞）受賞論文）. *岡山医学会雑誌* 2007; 119: 229—234.
7. 藤原俊義、田中紀章：微小癌転移の *in vivo* イメージング技術. ***Medical Science Digest*** 2008; 34: 48-49.

2. 学会発表

【国際学会】

1. Fujiwara, T., Urata, Y. Telomerase-specific oncolytic virotherapy for human cancer with hTERT promoter. ***15th International Conference on Gene Therapy of Cancer***、2007.
2. Fujiwara, T., Tanaka, N. Vector shedding and biodistribution following intratumoral delivery of adenoviral p53 (ADVEXIN) in patients with advanced non-small cell lung cancer. ***EMEA/ICH Workshop on Viral/Vector Shedding***、2007.
3. Kojima, T., Watanabe, Y., Hashimoto, Y., Sakai, R., Kuroda, S., Uno, F., Kagawa, S., Urata, Y., Tanaka, N., Fujiwara, T. Telomerase-specific virotherapy targeting lymph node metastasis of gastrointestinal cancer. ***10th Annual Meeting of American Society of Gene Therapy***, 2007.
4. Ouchi, M., Kawamura, H., Nagai, K., Urata, Y., Fujiwara, T. Antiviral activity of cidofovir against telomerase-specific replication-competent adenovirus, Telomelysin (OBP-301). ***10th Annual Meeting of American Society of Gene Therapy***, 2007.
5. Watanabe, Y., Hashimoto, Y., Kagawa, S., Kawamura, H., Nagai, K., Tanaka, N., Urata, Y., Fujiwara, T. Valproic acid (VPA) enhances the antitumor effect of telomerase-specific replication-competent adenoviral agent OBP-301 (Telomelysin) in human lung cancer cells. ***10th Annual Meeting of American Society of Gene Therapy***, 2007.
6. Hashimoto, Y., Teraishi, F., Watanabe, Y., Sakai, R., Kuroda, S., Kagawa, S., Urata, Y., Tanaka, N., Fujiwara, T. Assessment for antitumor activity of telomerase-specific oncolytic virotherapy in the hypoxic microenvironment. ***10th Annual Meeting of American Society of Gene Therapy***, 2007.
7. Kuroda, S., Fujiwara, T., Watanabe, Y., Hashimoto, Y., Kojima, T., Sakai, R., Ouchi, M., Uno, F., Onimatsu, H., Urata, Y., Kagawa, S., Tanaka, N., Fujiwara, T. Mutual sensitization with telomerase-specific oncolytic virotherapy and ionizing radiation in cytotoxic activity against human cancer. ***10th Annual Meeting of American Society of Gene Therapy***, 2007.

8. Kagawa, S., Watanabe, Y., Hashimoto, Y., Kojima, T., Uno, F., Kuroda, S., Urata, Y., Tanaka, N., Fujiwara, T. Antitumor effect of telomerase-selective oncolytic adenoviral agent OBP-301 (Telomelysin) in pleural dissemination of human malignant mesothelioma. ***12th World Conference on Lung Cancer***, 2007.
9. Kuroda, S., Fujiwara, T., Kagawa, S., Uno, F., Kojima, T., Urata, Y., Tanaka, N., Fujiwara, T. Mutual sensitization with telomerase-specific oncolytic virotherapy and ionizing radiation in cytotoxic activity against human cancer. ***12th World Conference on Lung Cancer***, 2007.

【国内学会】

1. 香川俊輔、日置勝義、宇野太、寺石文則、児島亨、酒井亮、黒田新士、田中紀章、藤原俊義：ヒト胃癌細胞に対する TRAIL 発現腫瘍溶解ウイルス療法. *第 79 回日本胃癌学会総会（ワークショップ）*、2007.
2. 児島亨、藤原俊義、渡邊雄一、橋本悠里、酒井亮、黒田新士、浦田泰生、宇野太、香川俊輔、田中紀章：消化器癌の微小リンパ節転移を標的とする新規ウイルス製剤 OBP-301 による治療開発. *第 107 回日本外科学会定期学術集会（シンポジウム）*、2007.
3. Fujiwara, T., Kagawa, S., Tanaka, N., Mizuguchi, H., Urata, Y., Theranostic application of telomerase-specific oncolytic adenoviral agents.*第 13 回日本遺伝子治療学会（Clinical Research Enterprise）*、2007.
4. 藤原俊義、浦田泰生、田中紀章：*In vivo* imaging of lymph node metastasis with telomerase-specific replication-selective adenovirus expressing *GFP* gene. *第 66 回日本癌学会学術総会（シンポジウム）*、2007.
5. 藤原俊義、浦田泰生、田中紀章：ナノバイオ・ウイルス製剤のがん診断・治療への応用. *第 45 回日本癌治療学会総会（シンポジウム）*、2007.
6. 香川俊輔、日置勝義、池田義博、児島亨、酒井亮、宇野太、寺石文則、橋本悠里、浦田泰生、田中紀章、藤原俊義：胃癌腹膜播種に対する TRAIL 発現 oncolytic adenovirus の抗腫瘍効果. *第 107 回日本外科学会定期学術集会*、2007.
7. 寺石文則、橋本悠里、児島亨、宇野太、香川俊輔、合地明、田中紀章、藤原俊義：切除不能 gastrointestinal stromal tumor (GIST)に対する制限増殖型アデノウイルス(Telomelysin)を用いた新規癌ウイルス療法の確立. *第 107 回日本外科学会定期学術集会*、2007.
8. Watanabe, Y., Hashimoto, Y., Kagawa, S., Kawamura, H., Nagai, K., Tanaka, N., Urata, Y., Fujiwara, T. Enhanced antitumor efficacy of telomerase-specific replication-competent adenoviral agent OBP-301 with valproic acid (VPA) in human lung cancer cells. *第 13 回日本遺伝子治療学会*、2007.
9. Hashimoto, Y., Teraishi, F., Watanabe, Y., Sakai, R., Kuroda, S., Kagawa, S., Urata, Y., Tanaka, N., Fujiwara, T. Assessment for antitumor activity of telomerase-specific oncolytic virotherapy in the hypoxic microenvironment. *第 13 回日本遺伝子治療学会*、2007.
10. 児島亨、渡辺雄一、橋本悠里、黒田新士、宇野太、香川俊輔、浦田泰生、田中紀章、藤原俊義：Telomerase-specific virotherapy targeting lymph node micrometastasis of human cancer. *第 66 回日本癌学会学術総会*、2007.
11. 岸本浩行、Zhao Ming、林克洋、浦田泰生、藤原俊義、Michael Bouvet、Robert M. Hoffman：Screening of RFP tumor cell lines for sensitivity to the telomerase-specific replicating adenovirus expressing GFP. *第 66 回日本癌学会学術総会*、2007.
12. 橋本悠里、寺石文則、渡邊雄一、河村仁、浦田泰生、田中紀章、藤原俊義：Telomerase-specific oncolytic virotherapy for human tumor cells in the hypoxic microenvironment. *第 66 回日本癌学会学術総会*、2007.
13. 毎田佳子、京哲、森紀子、坂口純子、水本泰成、橋本学、高倉正博、藤原俊義、井上正樹：Visualization of cancer cells with telomerase-specific replicating adenovirus and its application to cancer screening. *第 66 回日本癌学会学術総会*、2007.
14. 鬼松秀樹、河村仁、渡邊雄一、橋本悠里、大内正明、一丸大樹、永井勝幸、田中紀章、浦田泰生、藤原俊義：Preclinical characterization of OBP-301: in vitro and in vivo cytopathic activity with or without E3 region. *第 66 回日本癌学会学術総会*、2007.
15. 大内正明、河村仁、渡邊雄一、橋本悠里、鬼松秀樹、一丸大樹、永井勝幸、田中紀章、浦田泰生、藤原俊義：Antiviral activity of cidofovir against telomerase-specific replication-competent adenovirus, OBP-301 (Telomelysin). *第 66 回日本癌学会学術総会*、2007.
16. 黒田新士、藤原俊哉、児島亨、渡邊雄一、橋本悠里、宇野太、香川俊輔、浦田泰生、田中紀章、藤原俊義：Mutual sesitization with telomerase-specific oncolytic virotherapy and ionizing radiation in antitumor activity. *第 66 回日本癌学会学術総会*、2007.

研究成果の刊行に関する一覧表

雑誌

発表者氏名	論文タイトル名	発表誌名	巻号	ページ	出版年
Endo, Y., Sakai, R., Ouchi, M., Onimatsu, H., Hioki, M., Kagawa, S., Uno, F., Watanabe, Y., Urata, Y., Tanaka, N., Fujiwara, T.	Virus-mediated oncolysis induces danger signal and stimulates cytotoxic-T-lymphocyte activity via proteasome activator upregulation.	**Oncogene**	(in press)		2007
Hashimoto, Y., Watanabe, Y., Shirakiya, Y., Uno, F., Kagawa, S., Kawamura, H., Nagai, K., Tanaka, N., Kumon, H., Urata, Y., Fujiwara, T.	Establishment of Biological and Pharmacokinetic Assays of Telomerase-Specific Replication-Selective Adenovirus (TRAD).	**Cancer Science**	99	385-390	2008
Fujiwara, T., Urata, Y., Tanaka, N.	Telomerase-specific oncolytic virotherapy for human cancer with the hTERT promoter.	**Curr. Cancer Drug Targets**	7	191-201	2007
藤原俊義、田中紀章	GFP発現ウイルス製剤を用いた消化器癌微小転移の*in vivo*イメージングシステム.	医学のあゆみ	220	659-661	2007
藤原俊義、田中紀章	癌のウイルス療法.	外科治療	96	368-373	2007
藤原俊義、田中紀章	テロメラーゼ特異的ウイルス製剤の癌診断・治療への応用.	ゲノム医学	7	129-134	2007
藤原俊義、田中紀章	テロメラーゼ依存性腫瘍融解ウイルス製剤のがん診断・治療への応用.	日本臨床	65	1913-1922	2007

Oncogene (2007), 1–7

www.nature.com/onc

ORIGINAL ARTICLE

Virus-mediated oncolysis induces danger signal and stimulates cytotoxic T-lymphocyte activity via proteasome activator upregulation

Y Endo[1,2], R Sakai[1,2], M Ouchi[3], H Onimatsu[3], M Hioki[1,2], S Kagawa[1,2], F Uno[1,2], Y Watanabe[3], Y Urata[3], N Tanaka[1] and T Fujiwara[1,2]

[1]Division of Surgical Oncology, Department of Surgery, Okayama University Graduate School of Medicine, Dentistry and Pharmaceutical Sciences, Okayama, Japan; [2]Center for Gene and Cell Therapy, Okayama University Hospital, Okayama, Japan and [3]Oncolys BioPharma Inc., Tokyo, Japan

Dendritic cells (DCs) are the most potent antigen-presenting cells and acquire cellular antigens and danger signals from dying cells to initiate antitumor immune responses via direct cell-to-cell interaction and cytokine production. The optimal forms of tumor cell death for priming DCs for the release of danger signals are not fully understood. OBP-301 (Telomelysin) is a telomerase-specific replication-competent adenovirus that induces selective E1 expression and exclusively kills human cancer cells. Here, we show that OBP-301 replication produced the endogenous danger signaling molecule, uric acid, in infected human tumor cells, which in turn stimulated DCs to produce interferon-γ (IFN-γ) and interleukin 12 (IL-12). Subsequently, IFN-γ release upregulated the endogenous expression of the proteasome activator PA28 in tumor cells and resulted in the induction of cytotoxic T-lymphocytes. Our data suggest that virus-mediated oncolysis might be the effective stimulus for immature DCs to induce specific activity against human cancer cells.
Oncogene advance online publication, 5 November 2007; doi:10.1038/sj.onc.1210884

Keywords: adenovirus; telomerase; dendritic cell; uric acid; danger signal

Introduction

Dendritic cells (DCs) are the most important professional antigen-presenting cells and play a critical role in the induction of primary immune responses against tumor-associated antigens. Mature DCs express high levels of major histocompatibility complex (MHC) class I, II and co-stimulatory molecules such as CD80 and CD86, and secrete T-helper type-1 (Th1) cytokines such as interleukin (IL)-12 and interferon (IFN)-γ. DCs acquire endogenous maturation stimuli from dying cells as a danger signal when they capture cellular antigens. Lack of danger signals delays maturation of DCs and causes active suppression of DCs stimulatory capacity, leading to the induction of T-cell tolerance (Steinman *et al.*, 2000). Shi *et al.* (2003) have previously identified uric acid as a novel endogenous warning molecule capable of alerting the immune system within cell lysates. The uric acid activates DCs following relocation from the inside to the outside of injured cells and converts immunity from non-protective to protective. In fact, it has been reported that uric acid levels are elevated in tumors undergoing immune rejection and that the inhibition of uric acid production delays tumor regression (Hu *et al.*, 2004).

Viruses have evolved to infect, replicate in and kill human cells through diverse mechanisms such as direct cell death machinery and fairly brisk immune responses. We reported previously that telomerase-specific replication-competent adenovirus (Telomelysin, OBP-301), in which the human telomerase reverse transcriptase (hTERT) promoter element drives the expression of *E1A* and *E1B* genes linked with an internal ribosome entry site (IRES), induced selective E1 expression and efficiently killed human cancer cells, but not normal human fibroblasts (Kawashima *et al.*, 2004; Umeoka *et al.*, 2004; Taki *et al.*, 2005; Watanabe *et al.*, 2006). Although the precise molecular mechanism of OBP-301-induced cell death is still unclear, the process of oncolysis is morphologically distinct from apoptosis and necrosis. These findings led us to examine whether tumor cells killed by OBP-301 infection could stimulate DCs, thus enhancing the immune response.

In the present study, we compared three types of tumor preparations as a source of cell-derived antigen for the priming of DCs: virus-induced oncolysis, chemotherapeutic drug-induced apoptosis and necrosis by freeze/thaw. We also explored the cytokine signature and activating property of these cells for antitumor immune response against human cancer cells.

Results

We first examined whether OBP-301 infection affects the viability of human cancer cells using the XTT assay.

Correspondence: Dr T Fujiwara, Center for Gene and Cell Therapy, Okayama University Hospital, 2-5-1 Shikata-cho, Okayama 700-8558, Japan.
E-mail: toshi_f@md.okayama-u.ac.jp
Received 30 July 2007; revised 14 September 2007; accepted 17 September 2007

OBP-301 infection induced death of human cancer cell lines (H1299 human lung cancer and SW620 human colorectal cancer cells) in a dose-dependent manner (Figure 1). Although autophagy, or type II programmed cell death, partially involved in the cell death machinery triggered by OBP-301 infection, oncolytic cells are distinct from apoptotic cells (Supplementary Figure 1).

We next examined whether OBP-301 infection modulated intracellular concentrations of uric acid that might act as a danger signal in tumor cells. Uric acid levels increased in H1299 cells following OBP-301 infection in a time-dependent fashion, although docetaxel slightly upregulated the uric acid concentration 72 h after treatment (Figure 2a). Thus, tumor cells undergoing oncolysis can produce significantly greater amounts of uric acid when compared with apoptotic tumor cells. The uric acid elevation pattern of OBP-301-infected cells almost paralleled that of cells infected with Onyx-015, an E1B 55 kDa-deleted adenovirus engineered to selectively replicate in and lyse p53-deficient cancer cells, and wild-type adenovirus type 5 (Figure 2b), indicating a general effect of adenovirus infection in the regulation of intracellular uric acid levels.

Uric acid is produced during the catabolism of purines and is the end product of this process. Adenoviral replication facilitates the purine catabolism to stimulate the synthesis of progeny DNA, which in turn may increase intracellular uric acid levels by the purine degradation process. In fact, OBP-301 infection significantly increased the amount of uric acid in the cells, whereas replication-deficient dl312 infection had no apparent effect on the levels of uric acid. OBP-301-induced elevation of uric acid levels could be inhibited in the presence of cidofovir (CDV), an acyclic nucleoside phosphonate having potent broad-spectrum anti-DNA virus activity (Figure 2c). CDV has been approved for the treatment of many types of viruses including cytomegalovirus and adenovirus (Lenaerts and Naesens, 2006). We confirmed that CDV at 100 μM could significantly inhibited replication of OBP-301 in H1299 cells by the real-time quantitative PCR analysis (Supplementary Figure 2). Moreover, as OBP-301 replication was attenuated in telomerase-negative cells, the levels of uric acid could not be altered in normal human lung fibroblasts (NHLF) after OBP-301 infection (Figure 2d). These results suggest that viral replication is required to produce uric acid in infected cells.

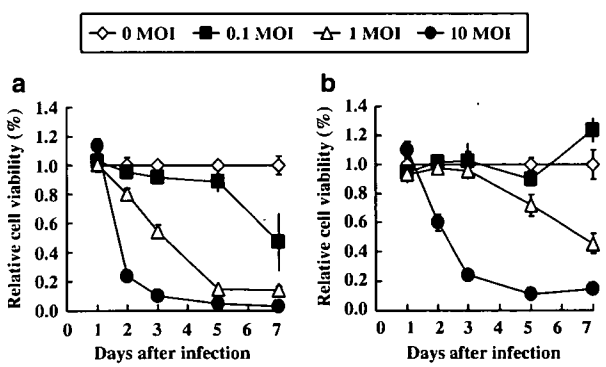

Figure 1 *In vitro* cytopathic effects of OBP-301 on human cancer cells. H1299 human non-small cell lung cancer (**a**) and SW620 human colorectal cancer cells (**b**) were infected with OBP-301 at indicated multiplicity of infection (MOI) values, and surviving cells were quantitated over 7 days by XTT assay. The cell viability of mock-treated cells on day 1 was considered 1.0, and the relative cell viability was calculated. Each data represent the mean ± standard deviation (s.d.) of triplicate experiments.

Xanthine oxidoreductase (XOR) is a member of the molybdoflavoenzyme family that catalyses the formation of uric acid from xanthine and hypoxanthine (Glantzounis *et al.*, 2005). A strand-specific reverse transcriptase PCR assay demonstrated that XOR mRNA expression gradually decreased in OBP-301-infected cells presumably due to the negative feedback of increased uric acid levels, whereas docetaxel-treated cells yielded consistent bands of the XOR transcripts (Figure 2e). Thus, adenoviral replication could directly stimulate the catalytic DNA turnover, which enables cells to produce more uric acid.

We then examined the ability of OBP-301-infected cells to stimulate immature DCs *in vitro*. DCs generated from HLA-A24$^+$ healthy volunteers were co-cultured with HLA-matched H1299 cells (HLA-A32/A24) treated with OBP-301 or docetaxel for 72 h, or freeze thawed. The production of Th1 cytokines such as IFN-γ and IL-12 in the supernatants was then explored by enzyme-linked immunosorbent assay (ELISA) analysis 48 h after the co-culture. DCs incubated with OBP-301-infected cells secreted large amounts of IFN-γ and IL-12, whereas stimulation with docetaxel-treated apoptotic cells induced their secretion at low levels (Figure 3a). The level of cytokine production from DCs incubated with freeze-thawed necrotic cells was similar to that of untreated immature DCs. Moreover, we confirmed that addition of OBP-301 alone without target tumor cells did not affect the cytokine secretion of DCs into the supernatant, indicating that infection of OBP-301 itself had no apparent effect on DCs. Thus, DCs stimulated with oncolytic tumor cells preferentially secrete high-level Th1 cytokines. Flow cytometry demonstrated that the increase in the expression of CD83, which is expressed on mature DCs, was slightly higher on DCs incubated with oncolytic cells than those with apoptotic or necrotic cells, indicating that oncolytic tumor cells seems to have a positive influence on DC maturation (Supplementary Figure 3).

In the next step, we investigated the effects of oncolytic tumor cells on T-cell activation in the presence of DCs. H1299 cells were infected with OBP-301 over 72 h, and then co-incubated with HLA-matched HLA-A24$^+$ peripheral blood mononuclear cells (PBMCs) for another 48 h in mixed lymphocyte tumor culture (MLTC). In other tests, H1299 cells were exposed to docetaxel for 72 h or freeze thawed, and then co-cultured with PBMCs. We examined the secretion of IFN-γ and IL-12 into the supernatants after MLTC for 7 days. Stimulation with OBP-301-infected cells induced the secretion of high levels of IFN-γ and IL-12 into MLTC supernatants, which was significantly higher

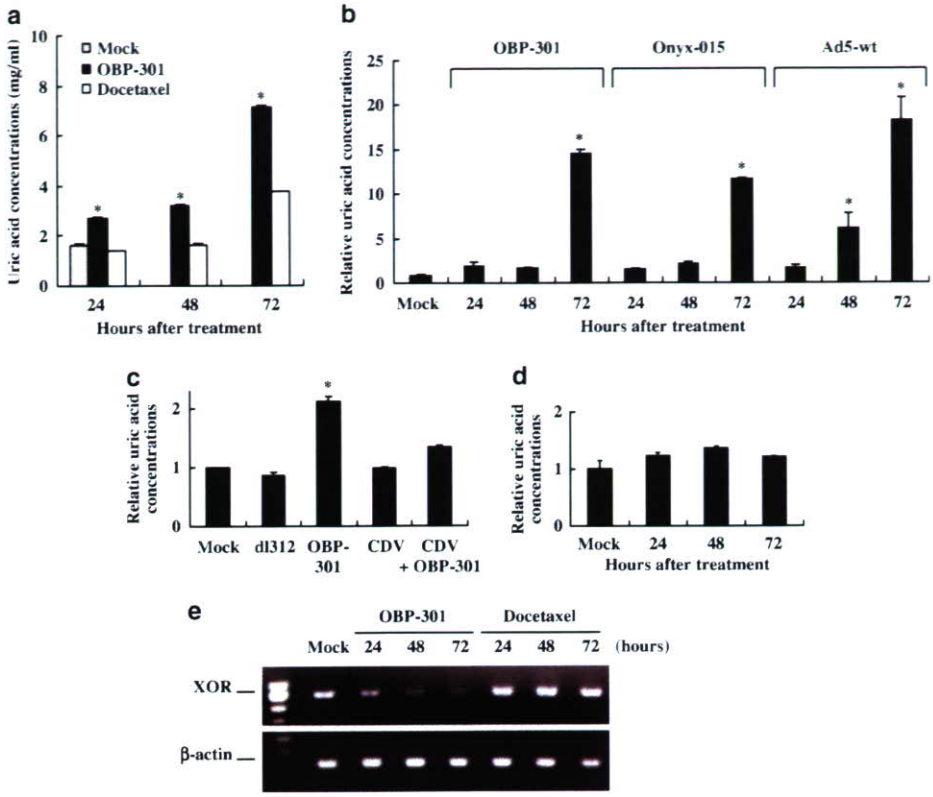

Figure 2 (**a**) Uric acid concentrations in H1299 cells treated with OBP-301 or docetaxel. H1299 cells were infected with 1.0 MOI of OBP-301 or treated with 10 nM of docetaxel for indicated time periods, and uric acid concentrations were determined enzymatically in the cell homogenates. Single asterisk indicates $P < 0.01$, significantly different from docetaxel-treated cells. (**b**) Uric acid levels in H1299 cells treated with OBP-301, Onyx-015 or wild-type adenovirus. H1299 cells were harvested at indicated time points over 72 h after infection with 10 MOI of viruses, and subjected to the measurement of uric acid concentrations. The levels of uric acid concentration are defined as the fold-increase for each sample relative to that of mock-treated cells (mock equals 1). Single asterisk indicates $P < 0.01$, significantly different from mock-treated cells. (**c**) Uric acid concentrations in H1299 cells infected with 1.0 MOI of OBP-301 or replication-deficient dl312 adenovirus were measured 24 h after infection. Uric acid production was also assessed in H1299 cells infected with 1.0 MOI of OBP-301 in the presence of 100 μM of anti-virus agent cidofovir (CDV). H1299 cells treated with 100 μM of CDV were subjected to the assay as a control. All uric acid levels are normalized to that of mock-treated cells (mock equals 1). (**d**) Uric acid levels in NHLF infected with OBP-301. NHLF cells were infected with 1.0 MOI of OBP-301 for indicated time periods, and uric acid concentrations were measured. The uric acid levels are normalized to that of mock-treated cells. (**e**) Detection of xanthine oxidoreductase (XOR) mRNA expression in OBP-301-infected H1299 cells by RT–PCR analysis. Cells were infected with 1.0 MOI of OBP-301 or treated with 10 nM of docetaxel, and then collected at the indicated time points. First-strand DNA generated from RNA was amplified using either the primers specific for XOR sequence or the primers that recognize β-actin sequences as an internal control.

than that with docetaxel-treated or freeze-thawed H1299 cells (Figure 3b). Thus, oncolytic tumor cells can accelerate the cleavage of tumor antigen peptides that can be associated with MHC class I molecules via IFN-γ secretion by immune cells.

Stimulation of cells with IFN-γ is known to induce the expression of PA28, a proteasome activator that accelerates the *in vitro* processing of MHC class I ligands from their polypeptide precursors (Sun *et al*., 2002). We investigated whether PA28 expression was upregulated in H1299 cells by adding the supernatants of co-cultures of PBMCs and OBP-301-infected H1299 cells. Western blot analysis for PA28 demonstrated that, following heat inactivation of residual OBP-301, MLTC supernatants with oncolytic tumor cells induced a strong endogenous PA28 expression in H1299 cells. In contrast, exposure to the supernatants of PBMCs alone, PBMCs with untreated H1299 cells, and PBMCs with oncolytic tumor cells without heat inactivation resulted in no apparent changes in the expression levels of PA28 (Figure 4).

Finally, the cytotoxic T-lymphocyte (CTL) response against human cancer cells was assessed by a standard 6-h ^{51}Cr release assay after a 7-day MLTC using various forms of H1299 cells. The lytic activity of CTLs induced by apoptotic or necrotic H1299 cells was comparable with that of human lymphokine-activated killer (LAK) cells; CTLs stimulated with oncolytic H1299 cells, however, more efficiently killed target H1299 cells (Figure 5). In contrast, LAK cells effectively lysed SW620 cells, whereas these cells were minimally killed by CTLs stimulated with apoptotic, necrotic or oncolytic H1299 cells. Furthermore, HLA-unmatched, HLA-A26/A30^{+} A549 human lung cancer cells were not sensitive to oncolytic tumor cell-induced cytotoxicity (data not shown), suggesting that effector cells stimulated with

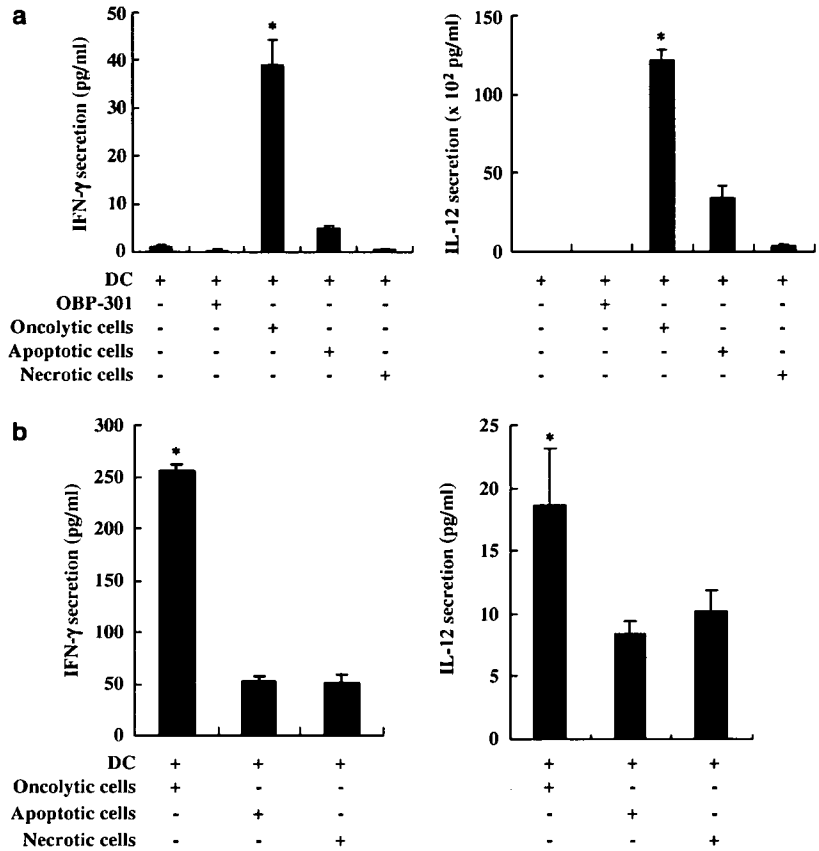

Figure 3 (**a**) Secretion of Th1-type cytokines by oncolytic, apoptotic or necrotic tumor cells. H1299 cells were treated with 1.0 MOI of OBP-301 or 50 nM of docetaxel for 72 h, or freeze thawed, and then co-cultured with immature dendritic cells (DCs) obtained from monocytes for additional 48 h. The culture supernatants were harvested and tested by ELISA for interferon (IFN)-γ (left) and interleukin (IL)-12 (right) concentrations. As a control, the supernatants of immature DCs alone or with OBP-301 at an MOI of 1.0 were also examined. Data are mean ± s.d. of triplicate experiments. Single asterisk indicates $P<0.01$, significantly different from other groups. (**b**) Tumor-specific CTL induction in MTLC with oncolytic, apoptotic or necrotic tumor cells. IFN-γ (left) and IL-12 (right) concentrations in the supernatants of MLTC analysed by ELISA. H1299 cells were treated with 1.0 MOI of OBP-301 or 50 nM of docetaxel for 72 h, or freeze thawed, and then co-cultured with PBMCs obtained from HLA-A24$^+$ healthy volunteers for 48 h in MLTC. Data are mean ± s.d. of triplicate experiments. Single asterisk indicates $P<0.01$, significantly different from other groups.

OBP-301-infected tumor cells exhibit MHC class I-restricted reactivity.

Discussion

In the present study, our goal was to determine whether oncolytic virus is effective not only as a direct cytotoxic drug but also as an immunostimulatory agent that could induce specific CTL for the remaining antigen-bearing tumor cells. Several groups have debated whether necrotic or apoptotic cells can stimulate DCs to cross-present cell-derived peptides, with subsequent enhancement of tumor immunogenicity. Furthermore, it has been reported recently that the immunogenicity of tumors is not regulated by signals associated with apoptotic or necrotic cell death, but is an intrinsic feature of the tumor itself (Bartholomae *et al*., 2004). Our data indicate that viral oncolysis could efficiently load tumor antigen on DCs, and then generate CTL response as judged from the production of cytokines. Moreover, the CTL activity against untreated tumor cells suggests that CTLs are specific to tumor antigens, but not to adenovirus proteins.

DCs are known to ingest dying tumor cells and initiate tumor-specific responses when associated with appropriate danger signals, which are endogenous activation signals liberated by dying cells. Recent studies have shown that some intrinsic biochemical factors, such as uric acid, bradykinin and heat shock protein (HSP110) act as danger signals through their interaction with DCs, and influence the subsequent immune response (Aliberti *et al*., 2003; Shi *et al*., 2003; Manjili *et al*., 2005). Large amounts of uric acid can be produced following tissue injury *in vivo*, and activate the immune response against injured cells and dying tissues. We found that OBP-301 infection increased intracellular uric acid levels in human tumor cells compared with apoptosis- or necrosis-inducing stimuli, suggesting that viral replication itself can enhance tumorigenicity.

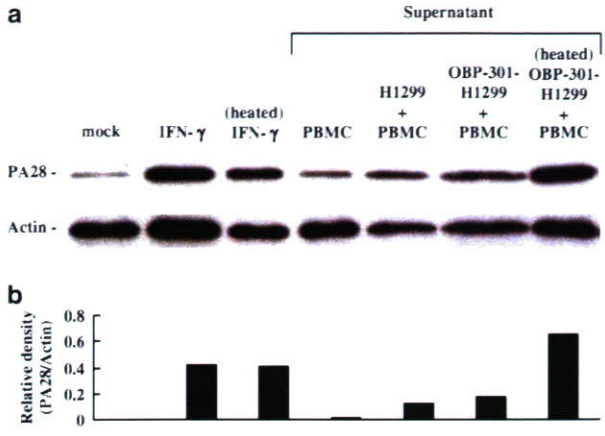

Figure 4 (**a**) Western blot analysis of PA28 in H1299 cells exposed to the supernatants of MLTC. peripheral blood mononuclear cells (PBMCs) were incubated with mock, untreated H1299 cells or H1299 cells treated with 10 MOI of OBP-301 for 72 h in MLTC, and the supernatants were harvested 48 h after the co-culture. H1299 cells were further incubated with the supernatants for 72 h with or without heat inactivation of residual virus (56 °C, 10 min). H1299 cells were also incubated with 5 ng ml^{-1} of interferon (IFN)-γ with or without heating for 72 h. Equivalent amounts of protein obtained from whole cell lysates were loaded in each lane, probed with anti-PA28 antibody and then visualized by using an ECL detection system. Equal loading of samples was confirmed by stripping each blot and reprobing with anti-actin antiserum. (**b**) PA28 protein expression was quantified by densitometric scanning using NIH Image software and normalization by dividing the actin signal.

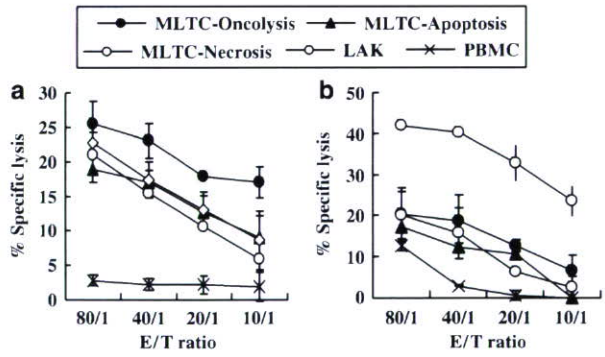

Figure 5 Cytolytic reactivity against H1299 (**a**) and SW620 (**b**) human cancer cells was assessed after 7-day mixed lymphocyte tumor culture (MLTC) with oncolytic, apoptotic or necrotic H1299 cells treated the same as above by 6-h standard ^{51}Cr-release assay. Lymphokine-activated killer (LAK) cells were generated from peripheral blood mononuclear cells (PBMCs) in the presence of interleukin (IL)-2 (100 U ml^{-1}) for 3 days. The CTLs were compared with LAK cells and untreated PBMCs, which served as positive and negative controls, respectively. Data represent the mean ± s.d. of three wells at four different effector-to-target (E/T) ratios.

Viral oncolysis increases the immunogenicity of tumor cells presumably by the release of proinflammatory cytokines (Lindenmann and Klein, 1967). We showed that OBP-301-infected oncolytic tumor cells efficiently stimulated immature DCs to produce greater amounts of IFN-γ and IL-12 than apoptotic and necrotic cells, and that such stimulation led to DC maturation. Viral infection itself has been reported to activate DCs to secrete pro- or anti-inflammatory cytokines, which can drive DCs to undergo the maturation process (Ho *et al*., 2001); the observation that OBP-301 alone had no effect on cytokine production by DCs, however, indicates that OBP-301 itself may be less infective or stimulatory to DCs. The result is consistent with our finding that OBP-301 attenuated replication as well as cytotoxicity in human normal cells.

It will be of interest to more mechanistically define why viral oncolysis efficiently induces CTL activity against tumor cells. We hypothesized that viral replication itself or the released cytokines by immune cells positively influences tumor cell immunogenicity. The IFN-γ-inducible proteasome modulator complex PA28 participates in the generation of antigenic peptides required for MHC class I antigen presentation (Sijts *et al*., 2002). As expected, the supernatants of MLTC with OBP-301-infected tumor cells, in which IFN-γ secretion was detected, induced a strong expression of endogenous PA28. Thus, oncolytic tumor cells can accelerate the cleavage of tumor antigen peptides that can be associated with MHC class I molecules via IFN-γ secretion by immune cells. In fact, it has been reported that restoration of PA28 expression in PA28-deficient melanoma cells rescues the melanoma antigen epitope presentation (Sun *et al*., 2002); our preliminary experiments however demonstrated that human tumor cells transfected with PA28α expression vector were less sensitive to tumor-specific CTLs (data not shown). These observations suggest that antigen peptide production alone does not seem sufficient to enhance tumor immunogenicity.

In conclusion, we provide for the first time evidence that oncolytic virus replication induces tumor-specific immune responses by stimulating uric acid production as a danger signal as well as accelerating tumor antigen cleavage by IFN-γ-inducible PA28 expression. Since the induction of systemic immunity has rarely been observed in clinical trials with other conditionally replication-competent viruses, more *in vivo* experiments are clearly required to support the induction of antitumor immunity by OBP-301 treatment. Our data, however, suggest that the antitumor effect of OBP-301 might be potentially both direct and indirect as well as systemic rather than local.

Materials and methods

Cell lines and reagents

The human non-small lung cancer cell lines H1299 (HLA-A32/A24) and the human colorectal carcinoma cell lines SW620 (HLA-A02/A24) were maintained *in vitro* in RPMI 1640 supplemented with 10% fetal calf serum, 100 U ml^{-1} penicillin and 100 mg ml^{-1} streptomycin. Recombinant human cytokines granulocyte/macrophage colony-stimulating factor (GM-CSF), IL-4, TNF-α and IL-7 were purchased from Genzyme

Techne (Minneapolis, MN, USA), IFN-γ from Peprotech (Rocky Hill, NJ, USA) and IL-2 from Roche (Mannheim, Germany). [^{51}Cr] sodium chromate was obtained from NEN Life Science Products (Boston, MA, USA). Docetaxel (taxotere) was kindly provided by Aventis Pharma (Tokyo, Japan).

Adenovirus
The recombinant replication-selective, tumor-specific adenovirus vector OBP-301 (Telomelysin), in which the hTERT promoter element drives the expression of *E1A* and *E1B* genes linked with an IRES, was constructed and characterized previously (Kawashima *et al.*, 2004; Umeoka *et al.*, 2004; Taki *et al.*, 2005; Watanabe *et al.*, 2006). Onyx-015 (dl1520) is an E1B 55 kDa-deleted adenovirus engineered to selectively replicate in and lyse p53-deficient cancer cells, and kindly provided by Dr Frank McCormick (UCSF Comprehensive Cancer Center and Cancer Research Institute). The E1A-deleted adenovirus vector lacking a cDNA insert (dl312) was also used as a control vector. The viruses were purified by $CsCl_2$ step gradient ultracentrifugation followed by $CsCl_2$ linear gradient ultracentrifugation.

Cell viability assay
XTT assay was performed to measure cell viability. Briefly, cells were plated on 96-well plates at 5×10^3 per well 24 h before treatment and then infected with OBP-301 or exposed to docetaxel. Cell viability was determined at the times indicated by using a Cell Proliferation Kit II (Roche Molecular Biochemicals) according to the protocol provided by the manufacturer.

Reverse transcription (RT)–PCR
Total RNA was isolated from mock-, OBP-301- and docetaxel-treated cells using RNAzol (Cinna/BioTecx, Friendswood, TX, USA) in a single-step phenol-extraction method and used as templates. Reverse transcription was performed at 22 °C for 10 min and then 42 °C for 20 min using 1.0 μg of RNA per reaction to ensure that the amount of amplified DNA was proportional to that of specific mRNA in the original sample. PCR was performed with specific primers in volumes of 50-μl according to the s protocol provided by the manufacturer (PCR kit; Perkin-Elmer/Cetus, Norwalk, CT, USA). The specific primers used for XOR were 5′-GCG AAG GAT AAG GTT ACT TGT-3′ (forward) and 5′-CTC CAG GTA GAA GTG CTC TTG-3′ (reverse); and for β-actin were 5′-ATG GTG GGA ATG GGT CAG AAG-3′ (forward) and 5′-GCA GCT CAT TGT AGA AGG-3′ (reverse). The reaction conditions were denaturing at 94 °C for 2 min followed by 30 cycles consisting of denaturing at 94 °C (30 s), annealing at 65 °C (15 s) and extension at 72 °C (10 s) using a thermal cycler (Perkin-Elmer, Foster City, CA, USA). The reactions were completed by a final 2-min extension at 72 °C. The PCR products were resolved on 1% agarose gels and visualized by SYBR Gold Nucleic Acid Gel Stain (Molecular Probes Inc., Eugene, OR, USA).

Preparation of tumor cells
For induction of oncolysis, tumor cells were infected with OBP-301 at a multiplicity of infection (MOI) of 1–10, and then collected 24–72 h after infection. Apoptotic tumor cells were obtained after 24–72-h exposure to 50–100 nM of docetaxel. For induction of necrosis, tumor cells suspended in phosphate-buffered saline (PBS) were subjected to rapid four freeze/thaw cycles using a 60 °C water bath and liquid nitrogen.

Measurement of uric acid concentration
Cultured cells were harvested after treatment and rinsed three times with PBS. These cells were resuspended in lysis buffer at a density of 200×10^6 cells per 100 μl. The buffer contained 10 mM Tris–HCl (pH 7.5), 150 nM NaCl, 50 mM NaF, 1 mM ethylenediaminetetraacetic acid (EDTA), 0.5 mM Na_3VO_4, 10% glycerol, 0.5% NP-40 and 0.1 mM phenylmethylsulfonyl fluoride (PMSF). After 10-s homogenization, the resulting extracts were kept on ice for 30 min and then were centrifuged for 15 min at 2000 *g*. The supernatants from treated tumor cells were assayed for uric acid using Uric Acid C test (Wako, Osaka, Japan).

Preparation of DCs
Peripheral blood samples were obtained from normal HLA-A24 positive healthy volunteers and PBMC were isolated by sedimentation over Ficoll-Hypaque. They were subsequently allowed to adhere in culture flasks for 1 h at 37 °C at a density of 4.0×10^7 cells per plate. Non-adherent cells in the plate were removed and the remaining (adherent) cells were cultured for 7 days in AIM-V (Gibco, Rockville, MD, USA) containing 2% heated-inactivated autologous serum supplemented with GM-CSF (50 ng ml^{-1}) and IL-4 (50 ng ml^{-1}).

Cytokine production assay
DCs were co-cultured with treated tumor cells at a ratio of 3:1 (DC/tumor cell) in a culture medium containing GM-CSF (50 ng ml^{-1}) and IL-4 (50 ng ml^{-1}). After 24-h incubation, the supernatant was collected and stored at −80 °C until the assay. The concentrations of IFN-γ and IL-12 (p40 and p70) were measured with appropriate ELISA kits (BioSource, Camarillo, CA, USA).

MLTC and CTL assay
PBMCs were co-cultured with treated tumor cells at a ratio of 20:1 in the presence of IL-2 (Roche) (10 U ml^{-1}) and IL-7 (Genzyme Techne) (5 ng ml^{-1}) for 7 days. Cultured cells were then used as effector cells in a standard 4 h-^{51}Cr release assay and the percentage of lysed cells was calculated. Percent specific lysis = ((experimental cpm − spontaneous cpm)/(maximal cpm − spontaneous cpm) × 100). Supernatants from MLTC performed as above were also assayed for IFN-γ and IL-12 by ELISA assays (BioSource).

Western blot analysis
The primary antibodies against proteasome activator PA28 (ZMD353; Invitrogen, Carlsbad, CA, USA), actin (AC-40; Sigma Chemical Co., St. Louis, MO, USA) and peroxidase-linked secondary antibody (Amersham, Arlington Heights, IL, USA) were used. Cells were washed twice in cold PBS and collected, then lysed in lysis buffer (10 mM Tris (pH 7.5), 150 mM NaCl, 50 mM NaF, 1 mM EDTA, 10% glycerol and 0.5% NP40) containing proteinase inhibitors (0.1 mM PMSF and 0.5 mM Na_3VO_4). After 20 min on ice, the lysates were spun at 14 000 rpm in a microcentrifuge at 4 °C for 10 min. The supernatants were used as whole cell extracts. Protein concentration was determined using the Bio-Rad protein determination method (Bio-Rad, Richmond, CA, USA). Equal amounts (50 μg) of proteins were boiled for 5 min and electrophoresed under reducing conditions on 6–12.5% (w/v) polyacrylamide gels. Proteins were electrophoretically transferred to a Hybond-polyvinylidene difluoride transfer membranes (Amersham Life Science, Buckinghamshire, UK), and incubated with the primary antibody, followed by peroxidase-linked secondary antibody. An Amersham ECL

chemiluminescent western system (Amersham) was used to detect secondary probes.

Statistical analysis

Data are expressed as mean ± s.d. The Student's *t*-test was used to compare differences. Statistical significance was defined when P was <0.05.

Acknowledgements

We thank Drs Tamotsu Yoshimori and Frank McCormick for providing pLC3-GFP plasmid and Onyx-015, respectively.

The study was supported by Grants-in-Aid from the Ministry of Education, Science and Culture, Japan; and Grants from the Ministry of Health and Welfare, Japan.

References

Aliberti J, Viola JP, Vieira-de-Abreu A, Bozza PT, Sher A, Scharfstein J. (2003). Bradykinin induces IL-12 production by dendritic cells: a danger signal that drives Th1 polarization. *J Immunol* **170**: 5349–5353.

Bartholomae WC, Rininsland FH, Eisenberg JC, Boehm BO, Lehmann PV, Tary-Lehmann M. (2004). T cell immunity induced by live, necrotic, and apoptotic tumor cells. *J Immunol* **173**: 1012–1022.

Glantzounis GK, Tsimoyiannis EC, Kappas AM, Galaris DA. (2005). Uric acid and oxidative stress. *Curr Pharm Des* **11**: 4145–4151.

Ho LJ, Wang JJ, Shaio MF, Kao CL, Chang DM, Han SW *et al.* (2001). Infection of human dendritic cells by dengue virus causes cell maturation and cytokine production. *J Immunol* **166**: 1499–1506.

Hu DE, Moore AM, Thomsen LL, Brindle KM. (2004). Uric acid promotes tumor immune rejection. *Cancer Res* **64**: 5059–5062.

Kawashima T, Kagawa S, Kobayashi N, Shirakiya Y, Umeoka T, Teraishi F *et al.* (2004). Telomerase-specific replication-selective virotherapy for human cancer. *Clin Cancer Res* **10**: 285–292.

Lenaerts L, Naesens L. (2006). Antiviral therapy for adenovirus infections. *Antiviral Res* **71**: 172–180.

Lindenmann J, Klein PA. (1967). Viral oncolysis: increased immunogenicity of host cell antigen associated with influenza virus. *J Exp Med* **126**: 93–108.

Manjili MH, Park J, Facciponte JG, Subjeck JR. (2005). HSP110 induces 'danger signals' upon interaction with antigen presenting cells and mouse mammary carcinoma. *Immunobiology* **210**: 295–303.

Shi Y, Evans JE, Rock KL. (2003). Molecular identification of a danger signal that alerts the immune system to dying cells. *Nature* **425**: 516–521.

Sijts A, Sun Y, Janek K, Kral S, Paschen A, Schadendorf D *et al.* (2002). The role of the proteasome activator PA28 in MHC class I antigen processing. *Mol Immunol* **39**: 165–169.

Steinman RM, Turley S, Mellman I, Inaba K. (2000). The induction of tolerance by dendritic cells that have captured apoptotic cells. *J Exp Med* **191**: 411–416.

Sun Y, Sijts AJ, Song M, Janek K, Nussbaum AK, Kral S *et al.* (2002). Expression of the proteasome activator PA28 rescues the presentation of a cytotoxic T lymphocyte epitope on melanoma cells. *Cancer Res* **62**: 2875–2882.

Taki M, Kagawa S, Nishizaki M, Mizuguchi H, Hayakawa T, Kyo S *et al.* (2005). Enhanced oncolysis by a tropism-modified telomerase-specific replication-selective adenoviral agent OBP-405 ('Telomelysin-RGD'). *Oncogene* **24**: 3130–3140.

Umeoka T, Kawashima T, Kagawa S, Teraishi F, Taki M, Nishizaki M *et al.* (2004). Visualization of intrathoracically disseminated solid tumors in mice with optical imaging by telomerase-specific amplification of a transferred green fluorescent protein gene. *Cancer Res* **64**: 6259–6265.

Watanabe T, Hioki M, Fujiwara T, Nishizaki M, Kagawa S, Taki M *et al.* (2006). Histone deacetylase inhibitor FR901228 enhances the antitumor effect of telomerase-specific replication-selective adenoviral agent OBP-301 in human lung cancer cells. *Exp Cell Res* **312**: 256–265.

Supplementary Information accompanies the paper on the Oncogene website (http://www.nature.com/onc).

Establishment of biological and pharmacokinetic assays of telomerase-specific replication-selective adenovirus

Yuuri Hashimoto,[1] Yuichi Watanabe,[1] Yoshiko Shirakiya,[1] Futoshi Uno,[2] Shunsuke Kagawa,[2] Hitoshi Kawamura,[1] Katsuyuki Nagai,[1] Noriaki Tanaka,[3] Horomi Kumon,[2] Yasuo Urata[1] and Toshiyoshi Fujiwara[2,4]

[1]Oncolys BioPharma, 3-16-33 Roppongi, Minato-ku, Tokyo 106-0031; [2]Center for Gene and Cell Therapy, Okayama University Hospital, 2-5-1 Shikata-cho, Okayama 700-8558; [3]Division of Surgical Oncology, Department of Surgery, Okayama University Graduate School of Medicine and Dentistry, 2-5-1 Shikata-cho, Okayama 700-8558, Japan

(Received June 25, 2007/Revised September 11, 2007/Accepted October 4, 2007/Online publication January 14, 2008)

The use of replication-selective tumor-specific viruses represents a novel approach for the treatment of neoplastic disease. We constructed an attenuated adenovirus, telomerase-specific replication-selective adenovirus (TRAD), in which the human telomerase reverse transcriptase promoter element drives the expression of the *E1A* and *E1B* genes linked with an internal ribosome entry site (IRES). Forty-eight hours after TRAD infection at a multiplicity of infection of 1.0, the cell viability of H1299 human lung cancer cells was consistently less than 50% and therefore this procedure could be used as a potency assay to assess the biological activity of TRAD. We also established a quantitative real-time polymerase chain reaction (PCR) analysis with consensus primers for either the adenovirus E1A or IRES sequence. The linear ranges of quantitation with E1A and IRES primers were 10^3–10^8 and 10^2–10^8 plaque-forming units/mL in the plasma, respectively. The PCR analysis demonstrated that the levels of *E1A* in normal tissues were more than 10^3 lower than in the tumors of A549 human lung tumor xenografts in *nu/nu* mice at 28 days after intratumoral injection. Our results suggest that the cell-killing assay against H1299 cells and real-time PCR can be used to assess the biological activity and biodistribution of TRAD in clinical trials. (*Cancer Sci* 2008; 99: 385–390)

The emerging fields of functional genomics and functional proteomics provide an expanding repertoire of clinically applicable targeted therapeutics.[1] Replication-selective oncolytic viruses provide a new platform for treatment of a variety of human cancers.[2,3] Promising clinical trials have shown the antitumor potency and safety of mutant or genetically modified adenoviruses.[4,5] We constructed previously an adenovirus vector, TRAD, in which the hTERT promoter element drives the expression of the *E1A* and *E1B* genes linked with an IRES. We showed that TRAD caused efficient selective killing of human cancer cells, but not normal cells.[6] Many studies have demonstrated that the majority of malignant tumors express telomerase activity,[7] suggesting that TRAD can potentially kill most human cancer cells.

TRAD can replicate and then lyse cancer cells, infect neighboring cancer cells, and subsequently induce oncolysis throughout the whole tumor mass *in vivo*. As preclinical models showed that TRAD could spread into the bloodstream, it is important to monitor carefully the amount of TRAD in the circulation after intratumoral injection of TRAD to avoid serious adverse events due to viremia. Although we used vector-specific primers that detected the p53 open reading frame–adenoviral DNA junction in a phase I clinical trial of a replication-deficient adenoviral vector expressing the wild-type *p53* gene (Advexin),[8] no appropriate method has been established to detect TRAD quantitatively. In addition, there is also a need for a procedure that can evaluate the biological activity of TRAD for clinical application.

In the present study, we characterized a potent antitumor viral agent, TRAD, to establish a biological assay and developed a single quantitative PCR method that can be used to assess the number of viral genomes present in the plasma as well as tissues.

Materials and Methods

Cells and culture conditions. H1299 (a human non-small-cell lung cancer cell line), H460 (a human large-cell lung cancer cell line), A549 (a human lung adenocarcinoma cell line), LNCap (a human metastatic prostate carcinoma cell line), MKN28 and MKN45 (human gastric adenocarcinoma cell lines), PC-3 (a human prostate adenocarcinoma cell line), SW620 (a human colorectal carcinoma cell line), and TE8 and T.Tn (human esophagus squamous carcinoma cell lines) were propagated to monolayer cultures in RPMI-1640 supplemented with 10% FBS, and 100 units/mL PG and 100 μg/mL SM. HeLa (a human cervical adenocarcinoma cell line), HepG2 (a human hepatocellular carcinoma cell line), Panc-1 (a human pancreatic epithelioid carcinoma cell line), and 293 (a transformed embryonic kidney cell line) were grown in DMEM containing high glucose (4.5 g/L) (high) with 10% FBS and PG/SM. HT-29 (a human colorectal adenocarcinoma cell line) was grown in McCoy's 5a with 10% FBS and PG/SM. MCF-7 (a human mammary gland adenocarcinoma cell line) was grown in Earle's Minimum Essential Medium with 10% FBS, PG/SM, and 2 mM L-glutamine. OST, SaOS2, and HOS (human osteosarcoma cell lines) were grown in DMEM (high) with 10% FBS and PG/SM. HSC-3 and HSC-4 (human tongue squamous carcinoma cell lines) were obtained from the Health Science Resources Bank (Osaka, Japan) and grown in DMEM (high) with 10% FBS and PG/SM. SCC-4 and SCC-9 (human tongue squamous carcinoma cell lines) were obtained from American Type Culture Collection (ATCC, Rockville, MD, USA) and grown in DMEM containing Nutrient Mixture (Ham's F-12) with 10% FBS, PG/SM, and 400 ng/mL hydrocortisone. U-2OS (a human osteosarcoma cell line) was obtained from ATCC and grown in McCoy's 5a with 10% FBS and PG/SM. NHLF was purchased from Takara Biomedicals (Kyoto, Japan) and cultured in the medium recommended by the manufacturer.

Recombinant adenoviruses. The recombinant replication-selective tumor-specific adenovirus vector TRAD was constructed and

[4]To whom correspondence should be addressed. E-mail: toshi_f@md.okayama-u.ac.jp

Abbreviations: ATCC, American Type Culture Collection; DMEM, Dulbecco's modified Eagle's medium; FBS, fetal bovine serum; hTERT, human telomerase reverse transcriptase; ID_{50}, the multiplicity of infection that causes 50% growth inhibition; IRES, internal ribosome entry site; NHLF, normal human lung fibroblasts; MOI, multiplicity of infection; PCR, polymerase chain reaction; PFU, plaque-forming units; PG, penicillin; SM, streptomycin; TRAD, telomerase-specific replication-selective adenovirus; XTT, sodium 3'-[1-(phenylaminocarbonyl)-3,4-tetrazolium]-bis(4-methoxy-6-nitro)benzene sulfonic acid hydrate.

doi: 10.1111/j.1349-7006.2007.00665.x

characterized as described previously.[6,9–11] The virus was purified by $CsCl_2$ step-gradient ultracentrifugation followed by $CsCl_2$ linear-gradient ultracentrifugation. The virus particle titer and infectious titer were determined spectrophotometrically and by plaque assay, respectively, in 293 cells.

Cell-viability assay. The XTT assay was carried out to measure cell viability. Cells were plated on 96-well plates at 1×10^3 cells/well 20 h before viral infection. HSC-4, SCC-4, and SCC-9 cells were then infected with TRAD at MOI of 0, 1, 10, and 50 PFU/cell. Other cell lines were infected with TRAD at MOI of 0, 0.1, 1, and 10 PFU/cell. Cell viability was determined at 1, 2, 3, and 5 days after virus infection using Cell Proliferation Kit II (Roche Molecular Biochemicals, Indianapolis, IN, USA) according to the protocol provided by the manufacturer. Using the cell viability data at 3 days after virus infection, we determined the TRAD ID_{50} of each cell line.

Cell-killing assay. H1299 cells were plated at 5×10^4 cells/well on 24-well plates and infected with TRAD at MOI of 0, 0.01, 0.1, 1, and 10 PFU/cell. Forty-eight hours later, the number of cells in each well was counted. Experiments were carried out in triplicate for each MOI, and cell viability was assessed by the trypan blue dye exclusion assay.

Quantitative real-time PCR assay. Viral DNA from serially diluted viral stocks and tumor cells infected with TRAD were extracted using QIAamp DNA Mini Kit (Qiagen, Valencia, CA, USA), and quantitative real-time PCR assay for either the *E1A* gene or the IRES sequence was carried out using a LightCycler instrument and a LightCycler DNA Master SYBR Green I kit (Roche Molecular Biochemicals). Typical amplification mixes (20 μL) contained 3 mM $MgCl_2$, 0.3 μM of each primer for IRES or 0.5 μM for *E1A*, and 2 μL of 10 × LightCycler FastStart DNA Master SYBR Green I. The sequences of the specific primers used in this experiment were: IRES, 5′-GAT TTT CCA CCA TAT TGC CG-3′ and 5′-TTC ACG ACA TTC AAC AGA CC-3′; E1A, 5′-CCT GTG TCT AGA GAA TGC AA-3′ and 5′-ACA GCT CAA GTC CAA AGG TT-3′. PCR amplifications were carried out in glass capillary tubes. PCR amplification for IRES began with a 10-min denaturation step at 95°C and then 40 cycles of denaturation at 95°C for 10 s, annealing at 60°C for 10 s, and extension at 72°C for 6 s. PCR amplification for *E1A* began with a 10-min denaturation step at 95°C and then 40 cycles of denaturation at 95°C for 10 s, annealing at 58°C for 15 s, and extension at 72°C for 8 s. Data analysis was carried out using LightCycler Software (Roche Molecular Biochemicals).

***In vivo* human tumor model.** A549 human lung cancer cells (5×10^6 cells/mouse) were injected subcutaneously into the flank of 7- to 9-week-old female BALB/c *nu/nμ* mice and permitted to grow to approximately 5–6 mm in diameter. At that stage, a 100-μL solution containing 1×10^8 PFU of TRAD was injected into the tumor. The tumors and organs were harvested 28 and 70 days later and DNA was extracted from each tissue. To compare viral replication in the tumor and other normal organs, quantitative real-time PCR for the *E1A* gene was carried out using a LightCycler instrument. The experimental protocol was approved by the Ethics Review Committee for Animal Experimentation of Okayama University School of Medicine.

Statistical analysis. All data were expressed as mean ± SD. Differences between groups were examined for statistical significance using Student's *t*-test. A *P*-value less than 0.05 denoted the presence of a statistically significant difference.

Results

***In vitro* cytopathic efficacy of TRAD in human cancer cell lines derived from different organs.** To determine whether TRAD infection induces broad-spectrum selective cell lysis, 23 tumor cell lines derived from 11 different organs (head and neck, lung, esophagus, stomach, colon, liver, pancreas, breast, prostate, uterus, and bone) were infected with TRAD at various MOI. Previous studies using a real-time reverse transcription-PCR method have demonstrated that these cell lines express detectable levels of hTERT mRNA.[6,9] Cytotoxicity was then assessed using the XTT cell-viability assay over 5 days after infection. As shown in Figure 1a, TRAD infection induced cell death in all cell lines except T.Tn esophageal cancer cells in a dose-dependent manner. Calculated ID_{50} values confirmed that all cell lines except T.Tn could be killed efficiently by TRAD at an MOI of less than 25 (Fig. 1b). These results suggest the broad-spectrum antitumor potency of TRAD.

Establishment of a standard assay to assess the biological activity of TRAD. H1299 human lung cancer cells and LNCap human prostate cancer cells were the most sensitive cell lines to TRAD-induced cell death (Fig. 1b). Accordingly, we used H1299 cells to evaluate the biological activity of TRAD. To test whether the selective replication of TRAD translates into selective oncolysis, we compared the cytopathic effects of TRAD in H1299 cells and NHLF at 5 days after infection. The dose–response curve of the relative cell viability in H1299 cells was shifted to the left compared to that in NHLF, suggesting that TRAD killed H1299 cells 10^2–10^3 more efficiently than NHLF (Fig. 2a).

We next determined the minimal dose of TRAD that could induce more than 50% of cell death in H1299 cells. As shown in Figure 2b, the cell viability of H1299 cells was less than 40% at 48 h after their infection with TRAD at a MOI of 1.0, but was 60% after infection with a MOI of 0.1. We also confirmed that H1299 cells at various passages (5th to 20th after purchase from ATCC) could be killed by TRAD in a similar fashion (data not shown). Therefore, TRAD could be considered biologically active, if TRAD at a MOI of 1 reduces the cell viability of H1299 cells by more than 50% at 48 h after infection. To estimate the utility of this assay, we examined the biological activity of heat-inactivated TRAD. Infection with intact TRAD at a MOI of 10 induced approximately 90% reduction in H1299 cell viability at 48 h after infection, whereas the antitumor activity was completely inhibited when it was preheated at 56°C for 5 or 10 min (Fig. 2c).

Development of quantitative PCR assay to detect copy numbers of TRAD. We used real-time PCR for quantitative detection of TRAD. Oligonucleotide primers were designed to achieve DNA amplification of the adenoviral E1A or IRES sequences in the TRAD genome (Fig. 3a). To generate accurate standard curves, TRAD at a known concentration was serially diluted and used as a template for real-time PCR analysis. Detection of IRES and E1A genome copies was achieved consistently and reproducibly by the PCR cycle values used. A linear relationship could be obtained between the number of cycles and the $\log_{10}$ dilution when 10^2–10^8 IRES copies and 10^3–10^8 E1A copies were assayed. Regression analysis of IRES and E1A curves resulted in very high correlation coefficients (0.99 and 1.00, respectively) for these concentration ranges (Fig. 3b). In addition, the dilution of TRAD virus in the plasma did not affect the sensitivity and dynamic ranges of quantification (Fig. 3b), suggesting that this method can be used to detect TRAD in the blood circulation.

***In vitro* quantification and replication monitoring of TRAD in infected human tumor and normal cells.** We next examined the replication ability of TRAD in different cell lines by measuring the relative amounts of IRES and E1A copy numbers. LNCap and NHLF cells were harvested at the indicated time points over 5 and 7 days, respectively, after infection with TRAD, and subjected to quantitative real-time PCR analysis using IRES and E1A primers. The ratios were normalized by dividing the value of cells obtained at 2 h after viral infection. As shown in Figure 4a, TRAD replicated 10^3–10^4 by 5 days after infection; its replication, however, was attenuated to less than 10^5 in normal NHLF cells. We previously reported that TRAD could replicate 10^5–10^6 by 3 days after infection in H1299 cells;[6,10] however, as

doi: 10.1111/j.1349-7006.2007.00665.x

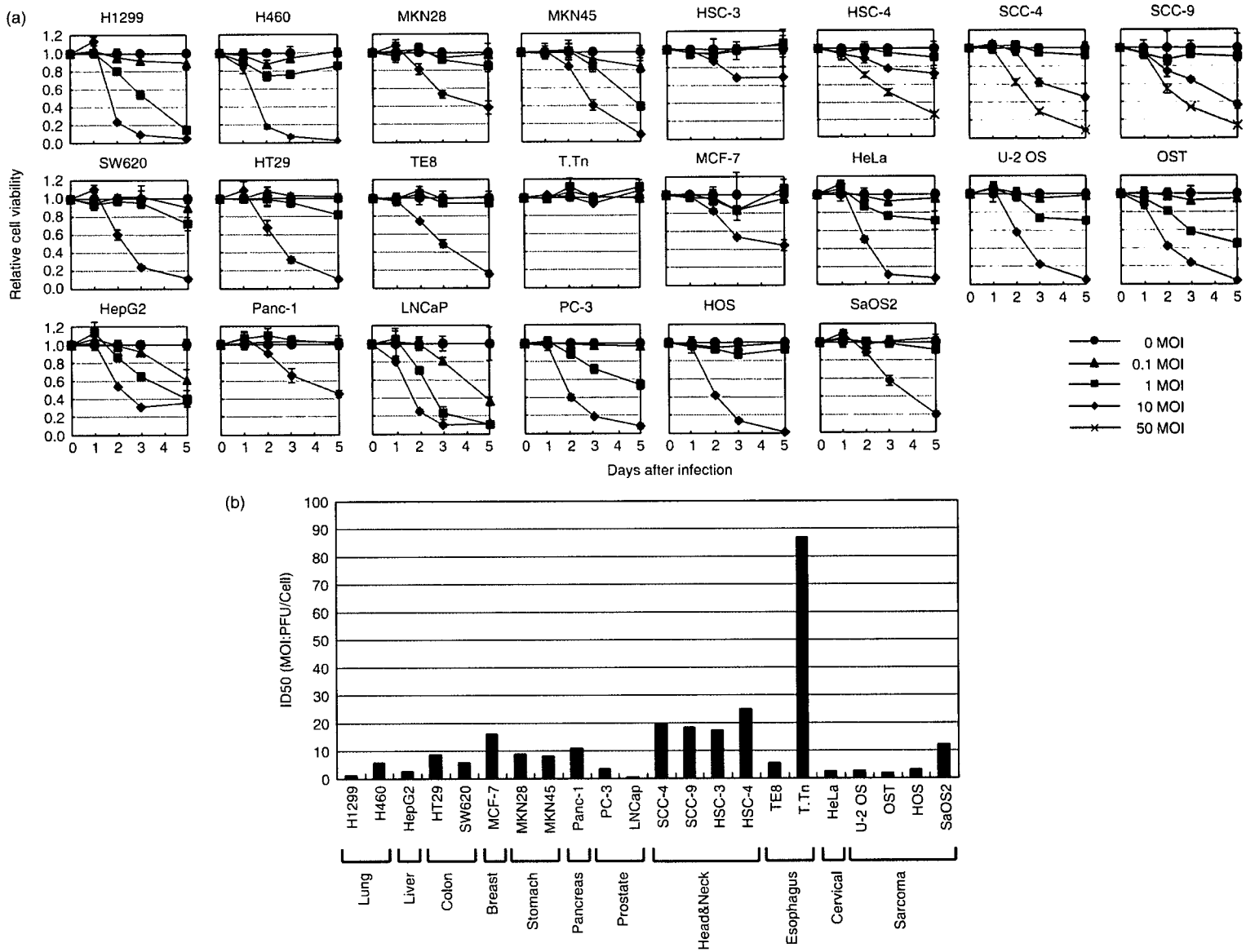

Fig. 1. Oncolytic effects of telomerase-specific replication-selective adenovirus (TRAD) *in vitro* on a variety of human cancer cell lines. (a) Cells were infected with TRAD at indicated multiplicity of infection (MOI) values, and surviving cells were quantitated over 5 days by XTT assay. Data are mean ± SD. (b) The 50% inhibiting doses of TRAD on cell viability at 3 days after infection were calculated and expressed as ID_{50} values. PFU, plaque-forming units; XXT, sodium 3′-[1-(phenylaminocarbonyl)-3,4-tetrazolium]-bis(4-methoxy-6-nitro)benzene sulfonic acid hydrate.

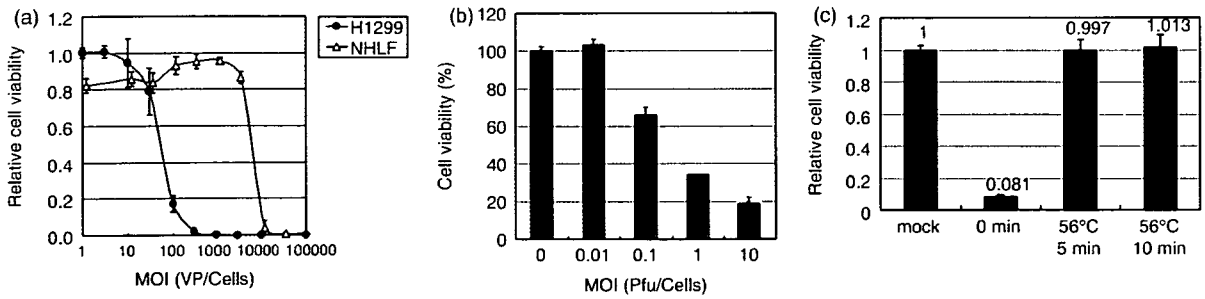

Fig. 2. Antitumor effects of telomerase-specific replication-selective adenovirus (TRAD) on H1299 non-small-cell lung cancer cells *in vitro*. (a) Effects of various concentrations of TRAD on H1299 cancer cells and normal human lung fibroblasts (NHLF) assessed at 5 days after treatment with XTT assay. Results are expressed as the percentage of untreated control. (b) H1299 cells were cultured as monolayers in triplicate in 24-well culture plates, infected with TRAD at the indicated multiplicities of infection (MOI), and assessed for cell viability 48 h after infection. Mock-infected cells were used as a control. (c) H1299 cells were plated on 96-well plates and infected with 10 MOI of TRAD heated at 56°C for 5 or 10 min, or non-treated TRAD. An XTT assay was carried out at 3 days after virus infection. Mock-infected cells were used as a control. Data represent the mean ± SD of triplicate experiments. PFU, plaque-forming units; XXT, sodium 3'-[1-(phenylaminocarbonyl)-3,4-tetrazolium]-bis(4-methoxy-6-nitro) benzene sulfonic acid hydrate; VP, virus particles.

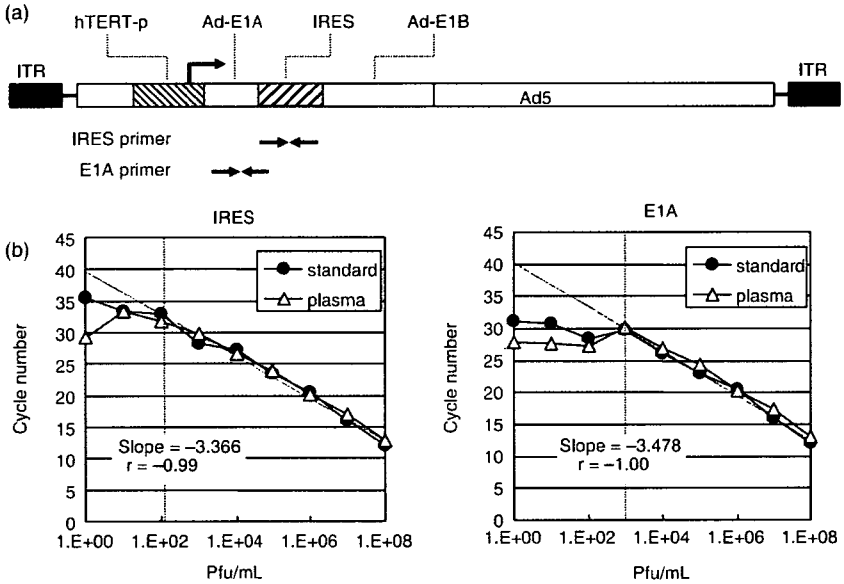

Fig. 3. Detection of normal human lung fibroblasts (TRAD) using quantitative polymerase chain reaction (PCR) assay. (a) Schematic diagram of the DNA structure of TRAD. TRAD contains the human telomerase reverse transcriptase (hTERT) promoter sequence inserted into the adenovirus genome to drive transcription of the *E1A* and *E1B* bicistronic cassette linked by the internal ribosome entry site (IRES) structure. Sites to which PCR primers (IRES and E1A) were targeted are indicated. Two primer pairs of IRES and E1A were designed to detect the TRAD genome. (b) Standard calibration curves of threshold cycle values and copy numbers are shown using serial dilution of TRAD virus stock. The coefficient of correlation (r^2) and slope are indicated for assays with IRES and E1A primers. ITR, inverted terminal repeats; PFU, plaque-forming units.

LNCap cells were more sensitive to TRAD-mediated cytotoxicity than H1299 cells (Fig. 1a), viral replication reached a plateau phase around 10^4 when LNCap cells started to die. Moreover, PCR targeting IRES and E1A showed similar replication profiles for TRAD in MCF-7 human breast cancer cells (Fig. 4b). To monitor the long-term viral replication, MCF-7 cells that were less sensitive to the cytopathic effect of the virus were used.

***In vivo* determination of TRAD genomes in tissue samples after intratumoral injection.** To evaluate selective replication of TRAD *in vivo*, we examined mouse tissues, including implanted tumors, for the presence of viral DNA by quantitative real-time PCR, following intratumoral viral injection. Mice with established subcutaneous A549 human lung tumor xenografts received a single intratumoral injection of 1×10^8 PFU of TRAD, and were killed 28 or 70 days after injection. To obtain the sufficient amounts of tumor tissues for analysis, we chose to use A549 cells. Our preliminary experiments demonstrated that intratumoral administration of TRAD suppressed tumor growth significantly compared with mock-treated tumors at 42 days after initiation of treatment ($P < 0.05$); however, the *in vivo* antitumor effect against A549 tumors was less than that against H1299 or LNCap tumors (data not shown). Although E1A DNA was detected in serum and some normal tissues examined (brain, heart, lung, ovary, liver, uterus, kidneys, bladder, colon, and axillary and mesenteric lymph nodes), tumors injected with TRAD contained at least 1000-fold more *E1A* copies (Fig. 5). These results suggest that quantitative real-time PCR allows detection and quantification of the number of TRAD genomes present in tissue samples after intratumoral injection of TRAD *in vivo*.

Discussion

Oncolytic viruses have been developed as anticancer agents based on the advantage of selective killing of tumor cells by controlled replication of the virus in the tumors, resulting in minimal undesired effects on normal cells.[2] Furthermore, amplified viruses can infect adjacent tumor cells as well as reach distant metastatic tumors through the blood circulation. Alhtough this might be a potential advantage of oncolytic viruses, systemic dissemination of large amounts of virus may induce virus-related symptoms including fever, diarrhea, pneumonia, and hepatitis, eventually leading to death. Therefore, virus shedding and distribution have to be evaluated by appropriate and suitable methods. In addition,

doi: 10.1111/j.1349-7006.2007.00665.x